CYBER
Pharmacodia AI

CYBER AIDD

WEEKLY REPORT

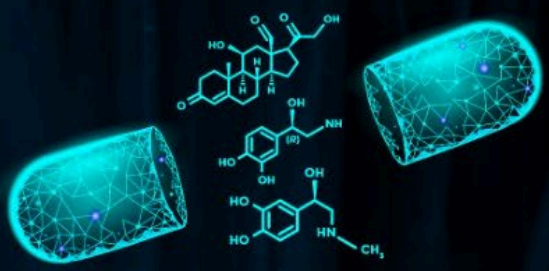

CyberAIDD assisted Analysis of Drug Discovery article titled Discovery of JNJ-748566665, A Novel isoquinolone DHODH inhibitor for treatment of AML developed by Johnson & Johnson.

(Reference: **J. Med. Chem. 2024, 67, 13, 11254–11272)**

CyberAIDD assisted analysis of Drug Discovery article titled Discovery of JNJ-748566665, A Novel isoquinolone DHODH inhibitor for treatment of AML developed by Johnson & Johnson

(Reference: **J. Med. Chem. 2024, 67, 13, 11254–11272)**

PART-I

Acute myeloid leukemia (AML) is a type of acute leukemia and is a hematologic malignancy. A range of isoquinolinone DHODH inhibitors were obtained through virtual screening and structure-based drug design approaches. The molecularly optimized DHODH inhibitor JNJ-748566665 with good physicochemical properties has been optimized for the clinical development of AML and myelodysplastic syndrome (MDS).

The CyberSAR System can provide in-depth elucidation of DHODH inhibitor molecules. The system shows the active molecules associated with the target through the cluster structure view and the original structure view, and presents the potential Hit in the form of a timeline of the R&D stage. In addition, CyberSAR also provides visual analysis of indications and trial design, helping developers quickly obtain target structure information and develop research ideas.

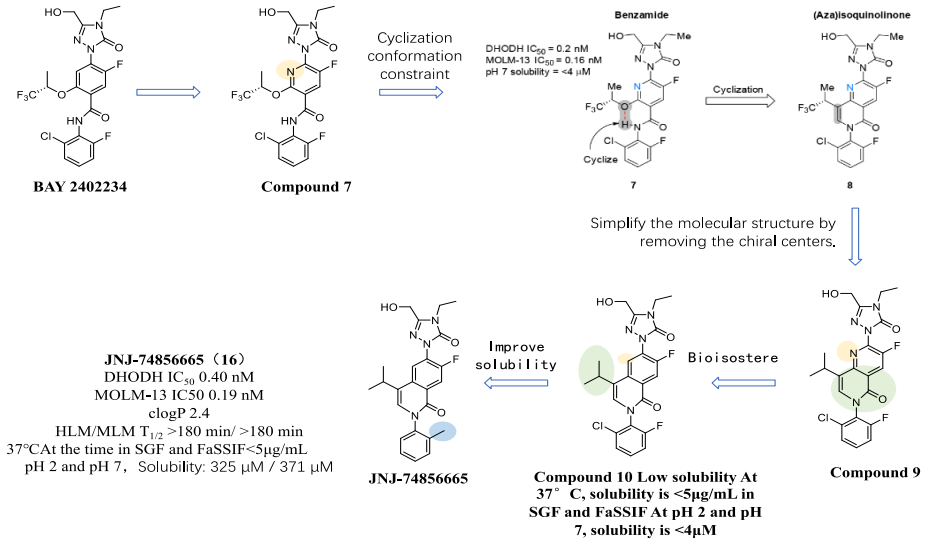

Figure 1. JNJ-74856665 discovery and molecular optimization process

Part II

Acute myeloid leukemia (AML) is a blood and bone marrow disease characterized by a lack of cell differentiation, causing a buildup of immature cells with the ability to self- renew. All-trans retinoic acid (ATRA) was initially used in clinical practice to treat AML, particularly acute promyelocytic leukemia (APL), a subtype of AML (10−15% of patients with AML). The recent use of ivosidenib (AG-120) and enasidenib (AG-221), selective inhibitors of mutant isocitrate dehydrogenase 1 or 2 (IDH1 and IDH2), respectively, for the treatment of AML, has resulted in durable remission in 8−12% of AML patients, and effective differentiation therapies for the broader population of AML patients are expected to significantly improve the treatment of the disease.

Dihydroorotate dehydrogenase (DHODH) is a key enzyme that converts dihydroorotate (DHO) to oroticacid (ORO) using the dehydropyrimidine synthesis pathway. This enzyme is a differentiated target in HOXA9-overexpressing leukemia cells and is considered the best target for unbiased phenotypic screening. HOXA9 is a key transcriptional regulator for stem cell maintenance and is normally expressed in hematopoietic progenitor cells but overexpressed in AML. The addition of exogenous uridine avoids DHODH inhibition by pyrimidine salvage pathway, thus confirming the mechanism of action of DHODH.

In vivo validation studies have shown that brequinar (2), a DHODH inhibitor, is able to overcome bone marrow differentiation blockade, reduce leukemia cell burden and leukemia initiating cells, and significantly improve the survival of preclinical AML models of different genetic subtypes. DHODH also exhibits excellent synthetic lethality sensitivity in several carcinogenesis. DHODH may have a synergistic effect as part of combination therapy for the treatment of patients with AML.

There is an urgent clinical need for next-generation DHODH inhibitors with higher specificity, potency, and favorable developmental properties. The adverse side effects of leflunomide (1) raise concerns about off-target activity beyond DHODH inhibition. Dose- limiting toxicities and minimal objective response rates in clinical studies in solid tumors make buquinaline unsuitable for clinical development. This is partly due to the general physicochemical properties, for example due to the presence of carboxylic acid groups in the molecular structure, which have an extremely high plasma protein binding rate and reduced cellular potency. A new generation of DHODH inhibitors comes from:

Multiple chemistically structured types, such as ASLAN003, BAY2402234, PTC299, and AG- 636 (Figure 1), have been used in the clinical development of refractory/relapsed AML, indicating widespread interest in DHODH as a differentiation target.

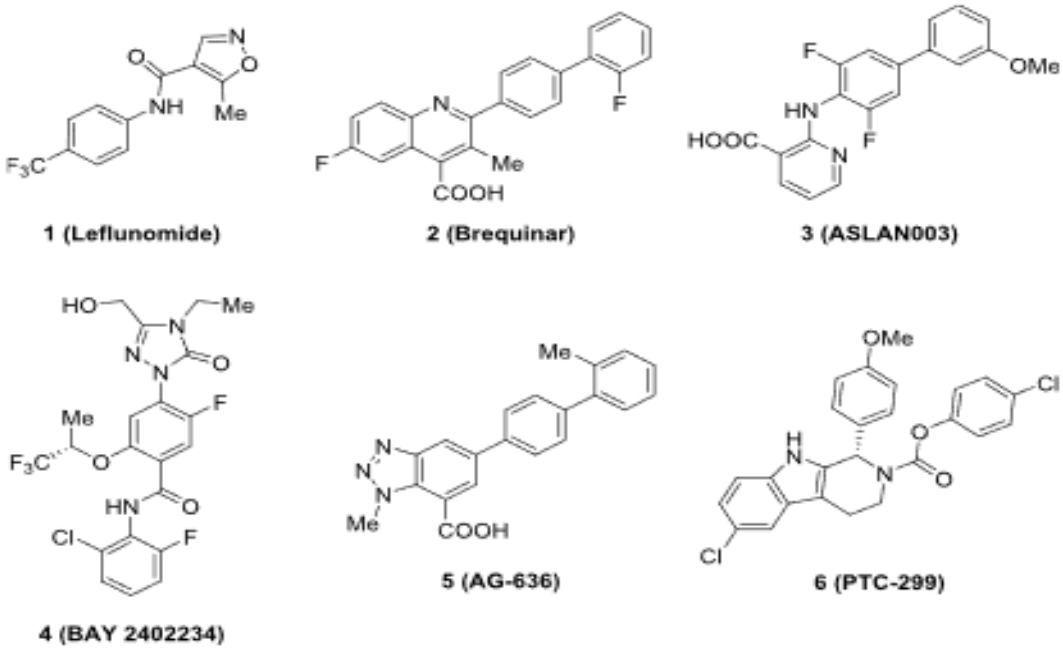

Figure 1. Chemical structures of clinical DHODH inhibitors.

Recently, Johnson & Johnson identified picolimide DHODH inhibitors, such as compound 7, by applying virtual screening and SBDD methods (Figure 2). This article describes the discovery and optimization of a novel (aza)isoquinolinone series derived from compound 7, which utilizes structure-based drug design to discover JNJ-74856665, a molecule with molecular properties suitable for clinical development. Eutectic structural analysis of compound 7 binding to human DHODH revealed that the formamide and the central pyridine ring are arranged in a planar arrangement mediated by intramolecular hydrogen bonds between the NH group and the ether oxygen atom (Figure 2).

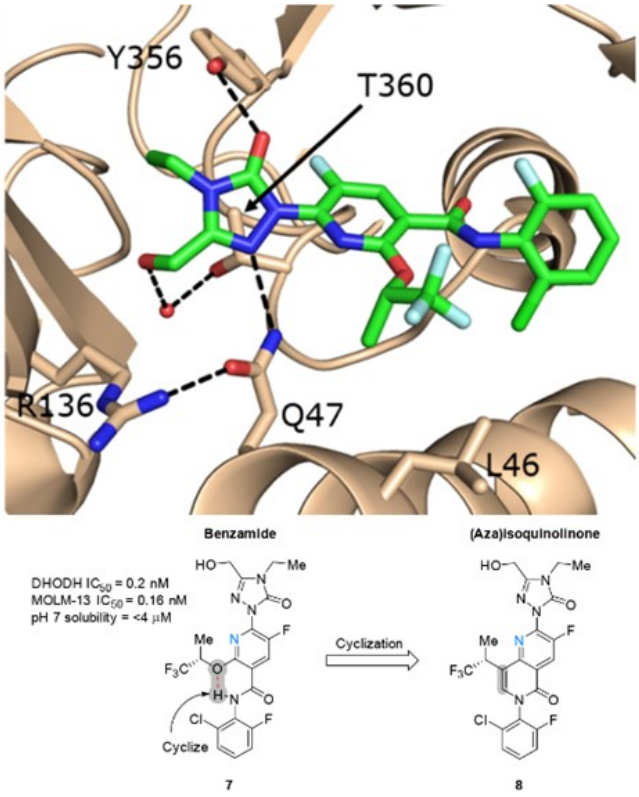

Figure 2. Putative DHODH inhibitor 8 with a fused six-membered ring by cyclization of compound 7. The cocrystal structure of compound 7 bound to human DHODH is also shown (PDB: 8DHF).

On the basis of this assumption, cyclization forms a six-membered bicyclic structure such as the azaisoquinolinone ring (the 1,6-naphtholinone ring of compound 8). Locking this putative molecular structure is expected to preserve key interacting and pharmacodynamic groups in the binding pocket. The conformational constraints resulting from the formation of ring structures by cyclization may have important effects on potency as well as physicochemical and ADME properties. After cyclization, it also prevents the release of 2-chloro-6-fluoroaniline in vivo through chemical bond cleavage or enzymatic cleavage of amide bonds. It was initially intended to concentrate on cyclized compound 7 to generate the azisoisoquilinones described above8, but it was ultimately decided to simplify by substituting trifluoromethylisopropyl ether with chiral isopropyl groups to speed up the initial synthesis and avoid chiral separation. Previous studies have shown that this substitute should still maintain potency in biochemical and cellular assays. The first compounds synthesized were azaquinolone9 and its quinolinone counterpart10 (Figure 3). By comparing the similar SARs of the corresponding pyridine in the central benzene ring and formamide series, it was found that the N and CH exchanges were bioelectronic isotropic.

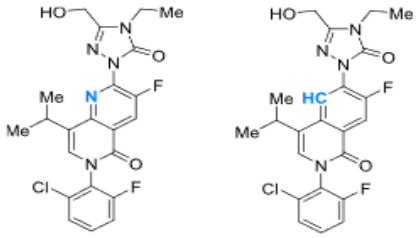

Figure 3. Chemical structures of initial isoquinolone analogues 9 and 10.

Human DHODH mediates the fourth redox step of the neopyrimidine biosynthesis pathway by catalyzing the oxidation of DHO to ORO. The inhibitory activity of 9 and 10 in human DHODH enzymes was evaluated using a photoabsorption assay with dichloroindifol (DCIP) as the definitive acceptor for the conversion of DHO to the hydride generated by ORO. Both 9 and 10 show excellent inhibition potency, with ICs of 0.36 nM and 0.22 nM, $_{50}$ respectively. 9 and 10 have antiproliferative activity in MOLM-13 cells of AML with ICs of 0.44 nM and 0.22 nM, $_{50}$ respectively. There is minimal variation between cellular potency and enzymatic potency for these compounds. Notably, the addition of excess uridine eliminated their antiproliferative activity (via the salvage pathway), suggesting that sub-nanomolar cellular potency comes from inhibition of DHODH. Finally, eutectic with a resolution of 2.1Å clearly shows the binding of compound 10 at the ubiquinone binding site of human DHODH, where the binding topology is consistent with the previously reported inhibitor. The overlap of this structure with 7-bound DHODH suggests that both compounds employ nearly identical binding patterns (Figure 4). The triazolone group of 10 is observed to form three hydrogen bonds at the more hydrophilic ends of the binding site. Specifically, hydrogen bonds are formed directly between the inhibitor and DHODH's Tyr356 and Gln47, as well as a water-mediated interaction with Thr360.

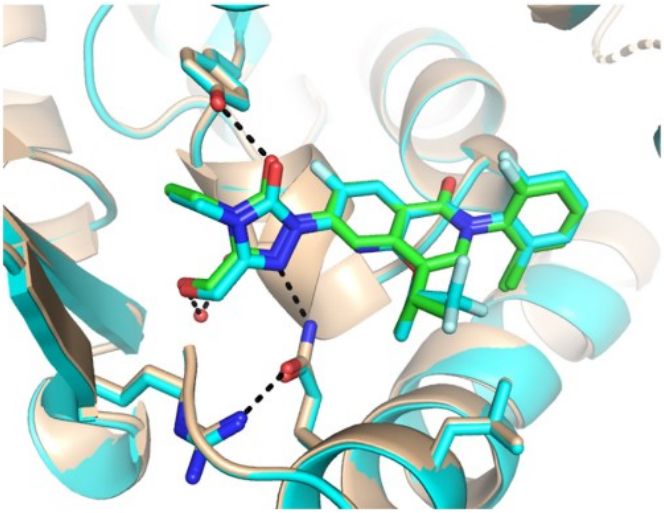

Figure 4. Cocrystal structure of compound **10** bound to the human DHODH ubiquinone pocket with 2.1 Å resolution overlaid with compound **7**. Dashed lines represent hydrogen bonds between **10** and DHODH (PDB: 9BKM).

After the isoquinolone backbone was identified as a valid replacement parent nucleus for acycloformamide, additional SAR exploration was performed. The area initially explored is isopropyl. Analogues 11, 12 and 13 were synthesized and evaluated in the DHODH enzymatic assay and the MOLM-13 cell assay (Table 1).

Table 1. Inhibitory Potency of Compounds 9–13 against Human DHODH and Anti-Proliferative Activity in AML MOLM-13 Cells

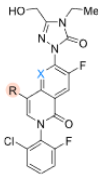

Compound	X	R	DHODH IC_{50} (nM)[a]	MOLM-13 IC_{50} (nM)[b]
9	N		0.36	0.44
10	CH		0.22	0.22
11	CH		0.27	0.10
12	CH		8.8	3.1
13	N		1.2	1.1

[a]Values represent the average of $n \geq 2$ experiments except for **12**, which was tested in a single experiment. Interassay variability <30%. DCIP absorbance assay has a LLOQ of 0.5 nM. [b]After a 72-h incubation (37 °C and 5% CO_2), cell viability was determined by adding CellTiter-Glo (Promega). Addition of excess uridine abrogated the antiproliferative activity for all compounds.

Isopropyl groups are found to be equivalent to isopropyl groups. For example, isoquinolinone 11 (DHODH IC $_{50}$ 0.27 nM; MOLM-13 IC $_{50}$ of 0.10 nM) and Homogener 10 (DHODH IC $_{50}$ of 0.22 nM; MOLM-13 IC $_{50}$ of 0.22 nM). The corresponding azaisoquilinone- 13 (DHODH IC $_{50}$ of 1.2 nM; MOLM-13 IC $_{50}$ of 1.1 nM) relative to its isopropyl
counterpart-9 (DHODH IC $_{50}$ of 0.36 nM; MOLM-13 IC $_{50}$). 0.44 nM) is less potent. These molecules were evaluated in assay experiments for the detection of reactive metabolites, and significant differences were observed. In the glutathione (GSH) capture experiment, compound 11 was positive, and two distinct glutathione conjugates (15.6%) were formed during human liver microsomal culture in the presence of GSH and NADPH, which were composed of P+O+GSH and P+2O+GSH. In contrast, reducing compound 10 did not contain such GSH adducts in the same experiment, suggesting that the isopropylene group may be responsible for the formation of reactive metabolites (Figure 5).

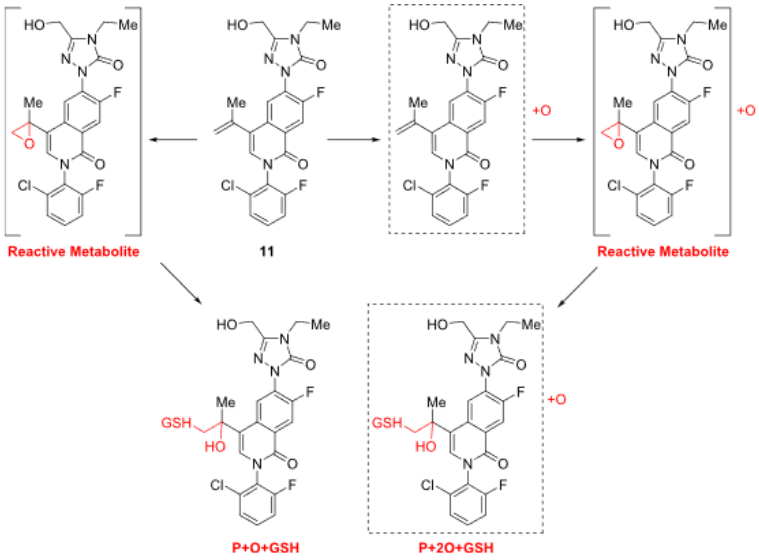

Figure 5. Proposed mechanism for the formation of two putative GSH adducts by in vitro incubation of compound **11** in human liver microsomes with GSH.

A putative bioactivation pathway is proposed, involving the initial stepwise oxidation or simultaneous epoxidation of isopropyl groups, followed by a nucleophilic attack by GSH, resulting in the formation of two putative GSH conjugates, P+O+GSH and P+2O+GSH. Attempts to block potential biological activity by introducing cyclopropyl groups can result in a loss of potency of more than 30-fold, as in compound 12.

Compound 10 was evaluated as an early lead in subcutaneous (sc) Human aml molm-13 xenografts. In vivo efficacy experiments, compound 10 exhibited significant dose-dependent tumor growth inhibition (>80% ΔTGI) in a female NSG mouse model of human AML MOLM-13 xenograft model 10 days after daily oral administration. However, the solubility of compound 10 was found to be extremely low (< 5 µg/mL in SGF and FaSSIF at 37°C), which was a potential problem for formulation development (Table 2).

In order to solve the solubility problem of compound 10, the modification focused on the substitution of the highly lipophilic 2-chloro6-fluorobenzene ring. Comparison with other desired parameters (e.g., solubility) can equilibrate the sub-nanomolar potency of compound 10 if necessary. This strategy has been shown to be effective in the early family of picolidinecarboxamides. As a first step, isoquinolinone analogues modified with a 2- chloro-6-fluorobenzene ring site were synthesized. Table 2 summarizes the potency, in vitro ADME, and physicochemical properties of the selected representative compounds.

Ortho-monosubstituted phenyl analogues were first examined as shown below14-20 (Table 2). The homologs have good stability in human and mouse liver microsomal assays in vitro ($T_{1/2}$ >180mins) and are highly permeable in MDCK-MDR1 cells. Using compound 10 as a starting point, the solubility was lower (<4 μM) as measured at pH 2 and pH 7 in a high-throughput equilibrium solubility experiment. The removal of chlorine atoms from compound 10 resulted in a more than 8-fold loss of potency for compound 15 (2.1 nM for 50 MOLM-13). Conversely, the removal of fluorine atoms from compound 10 maintained the same potency of compound 14 (0.28 nM IC_{50} for MOLM-13), but also improved solubility (155 μM, pH 7). The solubility (371 μM, pH 7) and equivalent compound 16 (0.19 nM IC_{50}) of MOLM-13 were further improved with methyl exchange compound 14 chlorine atoms. $_3$ Substitution of the methyl group of compound 16 with CHF_2 or CF results in a slight decrease in potency and a substantial loss of solubility, as in analogue 17 (0.56 nM IC_{50} for MOLM-13; solubility, 11 μM, pH7) and 18 (0.63 nM for $_{50}$ MOLM-13;

solubility, 39 μM, pH 7). The 2-methoxy analogue 19 (1.0 nM IC_{50} for MOLM-13; solubility,

20 μM, pH 7) and 2-ethyl homolog 20 (1.8 nM IC_{50} for MOLM-13; solubility, 157 μM, pH 7) did not show any improvement, confirming the superiority of 2-methyl in compound 16.

Notably, compound 14−20 has a very narrow lipophilic window (cLog P 2.1−2.9), but a wide range of solubility independent of lipophilicity can be observed with rather clever modifications.

Table 2. Inhibitory Potency in Human DHODH Enzyme and Anti-proliferative Activity in AML MOLM-13 Cells, ADME Parameters of 10 and 14–25

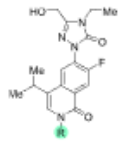

Compd	R	DHODH IC_{50} (nM)[a]	MOLM-13 IC_{50} (nM)[b]	cLogP[c] (LogD)	P_{app} A>B (+inh.)[d]	HLM /MLM $T_{1/2}$ (min)[e]	Sol pH2/7 (μM)[f]
10		0.22	0.22	2.8 (3.1)	24.5	>180/ >180	<4/ <4
14		0.42	0.28	2.7	50.7	>180/ >180	153/ 155
15		1.9	2.1	2.7	30.1	>180/ >180	19/ 19
16		0.40	0.19	2.4 (2.7)	33.1	>180/ >180	325/ 371
17		0.53	0.56	2.1	39.0	179/ >180	228/ 11
18		0.67	0.63	2.9	40.4	>180/ >180	NA/ 39
19		0.77	1.0	2.7	25.1	>180/ >180	19/ 20
20		1.2	1.8	2.9	37.3	>180/ 110	193/ 157
21		2.2	5.6	2.6	23.5	>180/ >180	235/ 189
22		0.46	0.67	2.6 (2.7)	48.2	>180/ >180	25/ 266
23		0.61	0.86	2.6	45.9	>180/ >180	30/ 30
24		0.44	0.69	2.6	47.4	>180/ >180	23/ 24
25	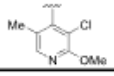	0.62	2.4	3.3	42.6	>180/ >180	78/ 21

[a]Values represent the average of $n \geq 2$ experiments except for 10 compounds, which were tested in a single experiment. Interassay variability <30%. DCIP absorbance assay has a LLOQ of 0.5 nM. [b]After a 72-h incubation (37 °C and 5% CO_2), cell viability was determined by adding CellTiter-Glo (Promega). Addition of excess amounts of uridine abrogated the antiproliferative activity for all compounds. [c]cLog *P* calculated using BioByte. [d]Passive permeability (cm/s × 10^{-6}) was measured from the apical (A) to the basolateral side (B) of MDCK-MDR1 cells in the presence of a P-gp inhibitor with recovery >60%. [e]For metabolic stability with HLM/MLM $T_{1/2}$: High stability >180 min; 33 min < medium stability <180 min; Low stability <33 min. [f]A high throughput solubility assay measured at pH 2 and pH 7.

Next, fluorine atom substitutions at different positions were explored under 2-methylbenzene ring compound 16, as shown in analogues 21−24. A significant decrease in the potency of 3-fluoride was observed in compound 21 (5.6 nM for $_{50}$ MOLM-13), but other combinations of fluorine in the presence of 2-methyl were tolerated, as shown in compound 22−24. 4-Fluoro-2-methyl analogue 22 (0.67 nM IC $_{50}$ for MOLM-13; solubility, 266 μM, pH 7) is more balanced in potency and solubility, but has no significant advantage over 16. In contrast, pyridyl analogue 25 showed improved solubility but reduced potency (2.4 nM IC $_{50}$ for MOLM-13; solubility, 21 μM, pH 7). In the previous series of pyridyl formamides, these heteroaryl analogues showed impressive potency, indicating a slight difference in SAR between the two series.

With the substitution of 2-methylphenyl by 2-chloro-6-fluorophenyl, analogue 16 acts as a lead compound, with significantly improved solubility and potency comparable to compound 10. To confirm that isopropyl is the optimal substituent, trifluoromethylisopropyl analogue53 was synthesized, (R)-enantiomer 26 was obtained by chiral SFC separation53, and absolute stereochemical accuracy was unambiguously confirmed by eutectic structure bound to human DHODH (PDB:9BKO). with (S)-enantiomer 27 (DHODH IC_{50} of 1.2 nM; 0.59 nM for MOLM-13) compared to 0.26 nM for compound 26 (DHODH IC_{50} ; MOLM-13 IC_{50} of 0.42 nM) has a 4-fold increase in potency in DHODH biochemical assays, but there is no significant difference in intracellular potency.
Compound 26 exhibits slightly lower potency (0.42 nM IC_{50} for MOLM-13) and lower solubility (181 μM, pH 7) in the cellular assay compared to compound 16 (0.19 nM IC_{50} for MOLM-13; solubility, 371 μM, pH 7), as shown in Table 3.

Compounds 16−19, 25, and 26 were evaluated in equilibrium solubility assays using simulated gastric juice (SGF, pH 1) and intestinal juice under fasting physiological conditions (FaSSIF pH 6.5). The crystal form of compound 16 exhibited moderate solubility (SGF, 25 μg/mL; FaSSIF, 67 μg/mL), but with a significant improvement in solubility compared to compound 10 (212 °C) (SGF, <5 μg/mL; FaSSIF, <5 μg/mL), which meets the lower melting point (164 °C). 17 (2-CHF_2) and 18 (2-CF_3) exhibit similar solubility ranges compared to compounds 16 with corresponding non-fluorinated 2-methyl substitutions. In contrast, 19, 25, and 26 all exhibited poor solubility (SGF, <5 μg/mL; FaSSIF，< 5 μg/mL）。
Notably, compound 26 is soluble in high-throughput assays (184 μM, pH 2; 181 μM, pH 7). This difference may reflect the fact that compound 26 remains amorphous in high-throughput assays, but becomes a more difficult to dissolve crystalline form after 24 hours of pulping. However, the results of the SGF and FaSSIF assays are thought to better reflect the low intrinsic solubility of compound 26.

In the single-dose PK study in mice (Table 4), 16, 18, 25, and 26 all exhibited exposures comparable to or greater than 10 after oral administration (AUC 71.8 μgh/mL, C_{max} 8.2 μg/mL). The clearance of all compounds was comparable to 10, and the oral bioavailability was >98%. In particular, compound 16 showed high exposure (AUC 57.2 μgh/mL, C_{max} 6.2 μg/mL) and had a good oral bioavailability of 125%. Although the trifluoromethylisopropyl ether group is optimal for the acycloformamide series, compound 26 has no significant advantage over achiral isopropyl 16. In terms of potency, solubility, and pharmacokinetic properties, the simpler isopropyl moiety is better for the isoquinolinone backbone.

Table 4. SGF, FaSSIF Solubilities, Human/Mouse Plasma Protein Binding (PPB) and Mean Single Dose PK Parameters of Compounds 10, 16, 18, 25, and 26 in C57BL Mice by PO and IV Dosing

compound	10	16	18	25	26
sol SGF (μg/mL)[a]	<5[e]	25[e]	17[f]	<5[f]	<5[f]
sol FaSSIF (μg/mL)[b]	<5[e]	67[e]	97[f]	16[f]	41[f]
human PPB (%)	95.8	90.1	93.7	94.1	90.0
mouse PPB (%)	97.6	91.2	93.3	96.2	90.7
CL (mL/min/kg)[c]	3.2	3.6	3.0	3.3	4.2
Vdss (L/kg)	1.3	1.6	1.2	2.1	1.3
$T_{1/2}$ (h)	5.1	5.7	4.3	7.0	4.0
C_{max} (μg/mL)	8.2	6.2	5.7	4.1	4.5
T_{max} (h)	0.83	1.7	1.3	1.5	1.5
$AUC_{(0\text{-}inf)}$ (μg h/mL)	71.8	57.2	71.1	82.5	39.0
F (%)[d]	135	125	127	109	98

[a]Media at 37 °C, pH 1. [b]Media at 37 °C, pH 6.5. [c]Mouse IV dose = 2 mg/kg, PEG400/water (70/30). [d]Mouse oral bioavailability (n = 3) dose 10 mg/kg, PEG400/water (70/30) vehicle. [e]Crystalline form. [f]Amorphous changed to crystalline form after slurrying for 24 h.

Co-crystallization of compound 16 with human DHODH enzyme showed the presence of three hydrogen bonds between the triazolone group in compound 16 and Tyr356, Gln47 and Thr360, similar to those seen in compound 10. The isoquinolone parent nucleus and 2-methylphenyl are associated with enzymes, especially with Tyr38, Met43, Leu46, Leu50, Ala55, Leu58, Phe62, Thr63, Leu67, Leu68, Leu359, and Pro364. The methyl group in the 2-methylphenyl group adopts a single conformation and points to the hydrophobic region in the pocket, as shown in Figure 6.

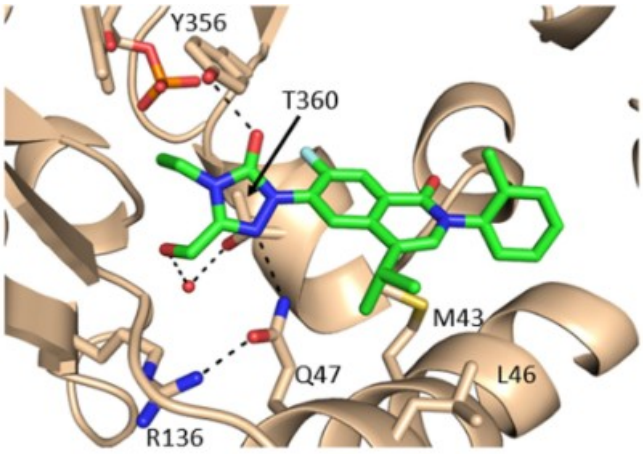

Figure 6. Cocrystal of compound **16** bound to human DHODH ubiquinone pocket with 1.3 Å resolution. Dashed lines represent hydrogen bonds between **16** and DHODH (PDB: 9BKN).

Taking into account all the data, compound 16 has the most balanced in vitro and in vivo pharmacological properties and is pending further evaluation. In mouse, rat, monkey, and human microsomes (all $T_{1/2}$ > 180 min), compound 16 cleared very slowly or undetectably in microsomal incubation. However, moderate clearance was shown in canine microsomes ($T_{1/2}$ was 57.5 min). Intrinsic clearance studies using cryopreserved hepatocytes also confirmed that compound 16 was stable in mice, rats, monkeys, and humans ($T_{1/2}$ > 371 min), but not in dogs ($T_{1/2}$ = 14.5 min) 。 In dogs, very high levels of O-glucuronic acid formation were observed (87%) vs 6% in other species. In microsomal and hepatocyte studies, liver clearance was highest in dogs and lowest in humans. In light of this result, cynomolgus monkeys were selected as a second species of non-rodents to replace dogs for safety studies. Compound 16 showed excellent PK parameters in cynomolgus monkeys, with low clearance (2.4 mL/min/kg) after a single IV dose, good exposure (AUC 64.6 μgh/mL, C_{max} 5.77 μg/mL), and excellent oral bioavailability (88%) after a 10 mg/kg dose orally as shown in Table 5, consistent with PK parameters in mice.

Table 5. Mean Single Dose PK Parameters of Compound 16 in Cynomolgus Monkey by PO and IV Dosing

IV dose (1 mg/kg)[a]			PO dose (10 mg/kg)[b]			
CL (mL/min/kg)	Vdss (L/kg)	$T_{1/2}$ (h)	C_{max} (μg/mL)	T_{max} (h)	$AUC_{(0\text{-inf})}$ (μg h/mL)	F (%)
2.4	1.2	6.4	5.8	3.3	64.6	88

[a]Solution in 70% PEG400/H_2O. [b]Suspension of crystalline form **16** in 0.5% hydroxypropyl methylcellulose (HPMC).

Compound 16 was systematically evaluated in an in vitro non-clinical safety assay. Compound 16 showed low CYP450 inhibition (all $_{50}$ ICs >20 μM) measured against CYP450 isomer-specific substrates in human liver microsomes (HLM). No activation of aryl hydrocarbon receptor (AhR) (<-fold compared to vehicle control DMSO) was observed at in vitro concentrations of 1 μM and 10 μM in the CYP-inducible experimental assay, and leflunomide (1), a well-known DHODH inhibitor, is also an AhR activator.

Activation of PXR16 is observed at 1 μM (3.2-fold relative to vehicle control DMSO) and 10 μM compound concentrations (7.4-fold relative to vehicle-control DMSO), suggesting the potential for CYP3A4 induction. However, modest induction of CYP3A4 enzyme activity (midazolam hydroxylation to 1-hydroxymidazolam) was observed at 10 μM (2.5 times compared to vehicle control DMSO) in cryopreserved human hepatocytes, but not at 1 μM (<2x vehicle control DMSO). As a percentage of CYP3A4 induction control (10 μM rifampicin), enzyme activity is 7.3% at 1 μM and 20% at 10 μM. All these data suggest that based on compound 16 there is little to no CYP inhibitory activity, it is unlikely to be a perpetrator of drug-drug interactions (DDIs). Further studies (data not shown) have shown that compound 16 is primarily metabolized by CYP3A4 and care needs to be taken to avoid drug-drug interactions caused by concomitant administration of CYP3A4 inducers or inhibitors.

In vitro safety pharmacology assessment CEREP experiment, compound 16 had no significant interaction with hERG, Ca, $^{2+}$ and Na $^{+}$ ion channels, and all had $_{50}$ ICs >10 μM. In the secondary pharmacological CEREP group, compound 16 exhibits only inhibition of kappa opioid receptors (KOP, 96% at 10 μM); However, a follow-up study of a definitive KOP inhibition study showed $_{50}$ an IC of 14 μM. Compound 16 exhibits less than 50% inhibition of 468 wild-type and mutant kinases (DiscoveRx) at 1 μM, with the exception of WNK2 (51%).

Sensitive surface plasmon resonance assay (SPR) using human DHODH protein is used to determine the binding kinetics and affinity of compound 16 with a dissociation constant or affinity: K_D of 2.22 nM and a half-life $t_{1/2}$ =19.7 min. The results are consistent with its affinity IC_{50} of 0.4 nM for the light-absorbing DHODH assay. Compound 16 potently inhibits the proliferation of a panel of AML cell lines with ICs_{50} in the sub-low nanomolar range, inducing differentiation, cell cycle arrest, and apoptosis. In the presence of excess uridine, all of these phenotypes can be avoided, consistent with the targeted mechanism of de novo pyrimidine synthesis blockade.

In MOLM-13 human AML xenografts established in female NSG mice, the in vivo efficacy of compound 16 was evaluated over 10 days (Figure 7). MOLM-13 tumors have a significant response to treatment with daily oral doses of 0.031, 0.062, 0.125, or 0.25mg/kg of compound 16, resulting in statistically significant tumor growth inhibition of 42%, 75%, 92%, or 93% ΔTGI in a dose-dependent manner.

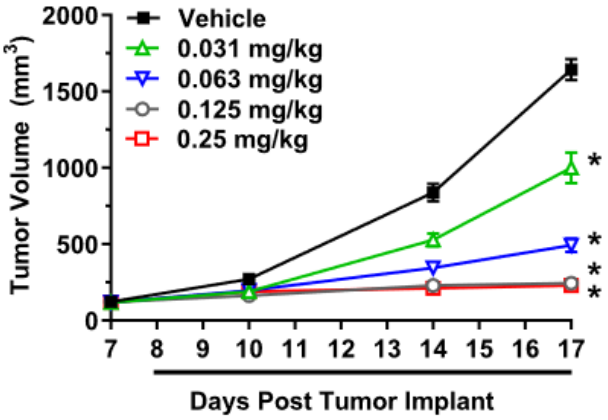

Figure 7. Oral in vivo efficacy profile of compound **16** in a MOLM-13 human AML xenograft model. Group tumor volumes are graphed as mean ± SEM (standard error of the mean) (n = 10/group). Tumor cells were implanted on Day 0 and treatment occurred on Days 8−17 for a total of 10 doses, as denoted by the horizontal bar below the X-axis. Data is displayed to Day 17 of treatment when control mice were removed from study. *Denotes significant difference ($p \leq 0.05$) from the vehicle control group calculated over time through Day 17.

After long-term treatment, all of these doses of compound 16 were tolerated. Mice show modest weight loss during the 10-day treatment period, but appear healthy. Using preclinical species PK parameters, the allometric scaling method predicted that compound 16 had a human systemic clearance of 0.89 mL/min/kg and a distribution volume (steady state) of 0.88 L/kg. PK parameters, assuming bioavailability of 100% to 60%, respectively, would expect an effective human dose between 3 and 5 mgQD for 90% ΔTGI.

This article describes the discovery and optimization of a series of isoquinolone DHODH inhibitors with unique structural characteristics. Compound 16 (JNJ-74856665) has been designated as a clinical-stage DHODH inhibitor based on comprehensive preclinical data. JNJ74856665 is an orally bioavailable, potent, and highly selective DHODH inhibitor that is currently in clinical development for the treatment of acute myeloid leukemia and myelodysplastic syndrome (NCT04609826).

Reference Article from: https://doi.org/10.1021/acs.jmedchem.4c00809
J. Med. Chem. 2024, 67, 13, 11254–11272

Part III

1. Combined with drug design ideas, CyberSAR excavates the active structure reported in the literature and patents, and uses CyberSAR to quickly obtain the target structure of interest of R&D personnel for developing ideas, and DHODH (Homo sapiens) is an example as follows:

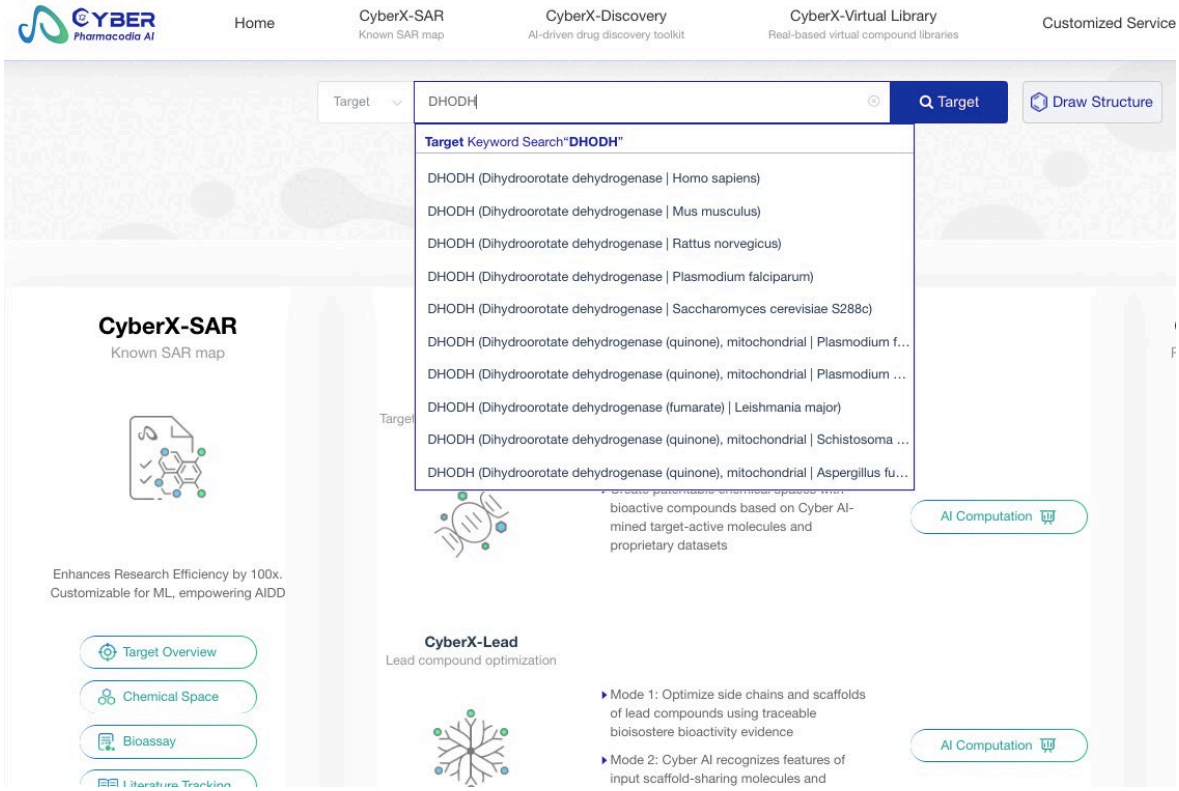

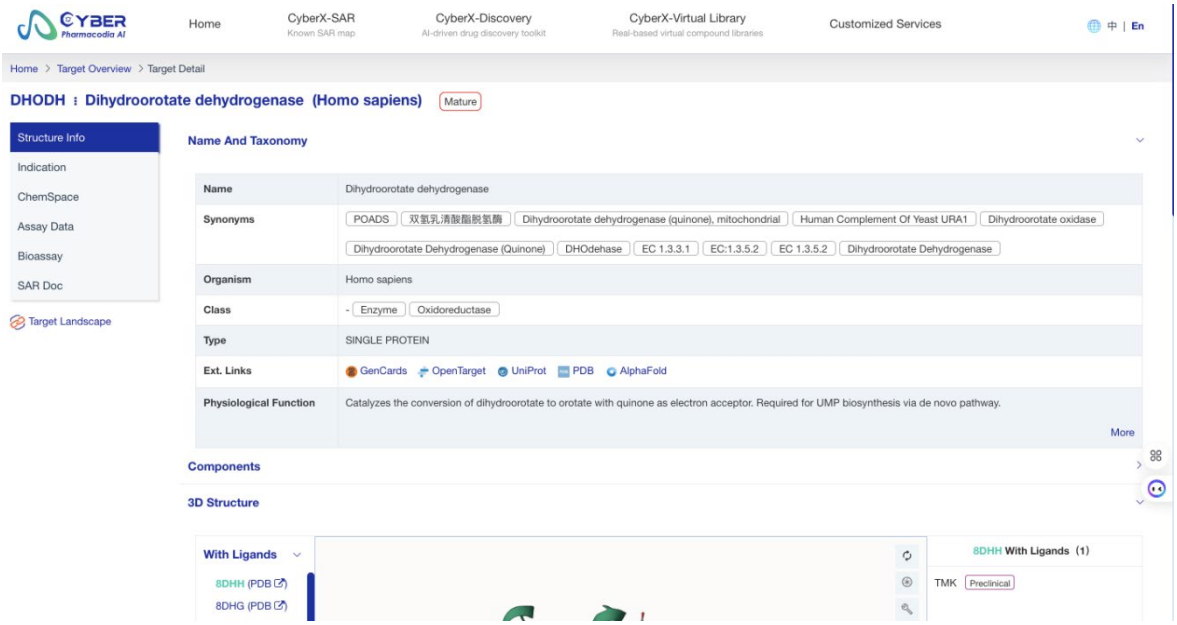

2. The PDB code of the eutectic structure of "DHODH (Homo sapiens)" and the corresponding ligand small molecule structure are included in the target interface, which can efficiently and conveniently obtain the ligand small molecule structure and interaction mode in the eutectic structure of the target.

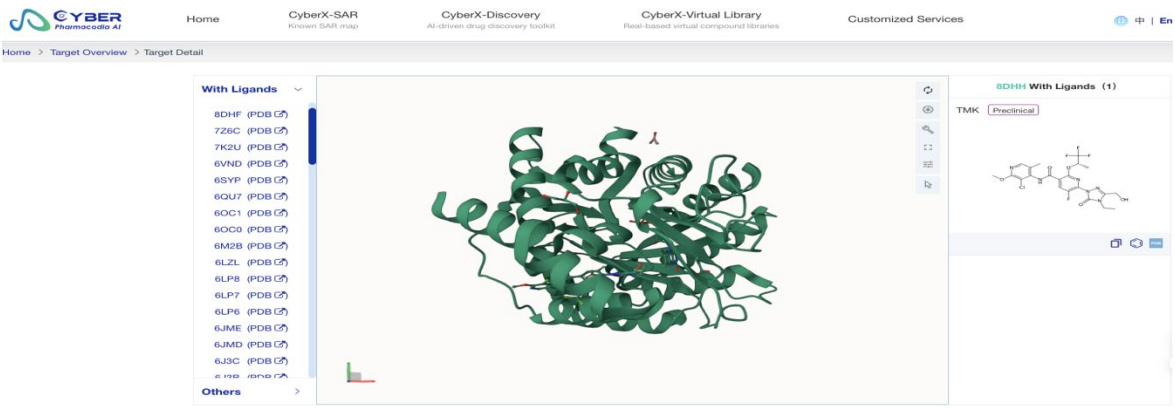

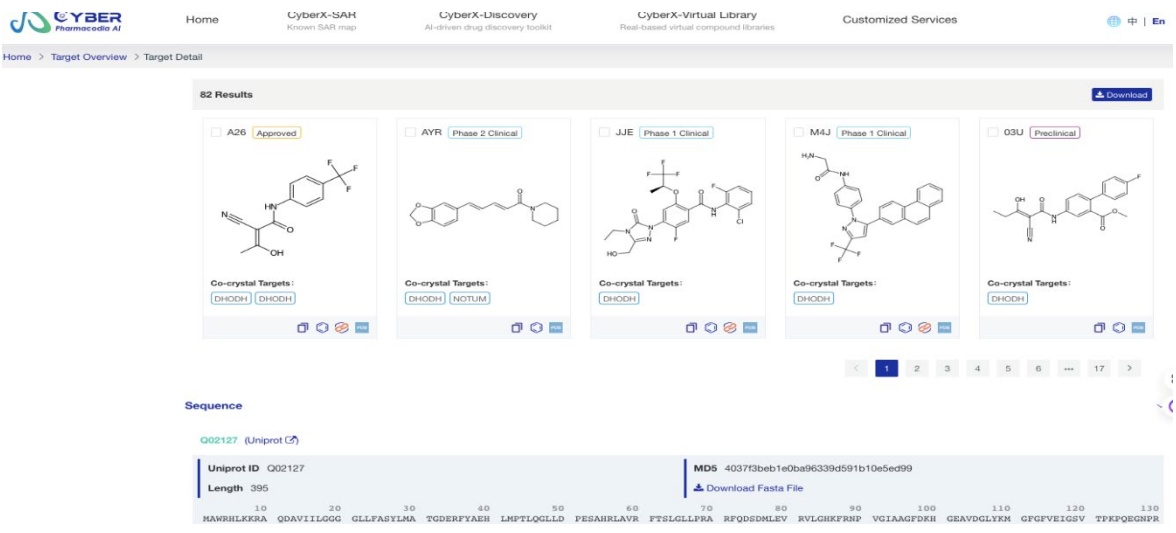

3. Select the "Cluster Structure View" tab under the "Chemical Space" option tab in the target interface, and the literature and patents included in the CyberSAR platform can display the molecules with experimental test activity related to DHODH (Homo sapiens) in the form of "parent nuclear structure clustering". Among them, the "highlighted" in green font is the active molecular structure of IC $_{50}$ <1000 nM in the in vitro enzyme and cell activity test experiments reported in the literature, the specific experiment, the experimental results and the experimental source.

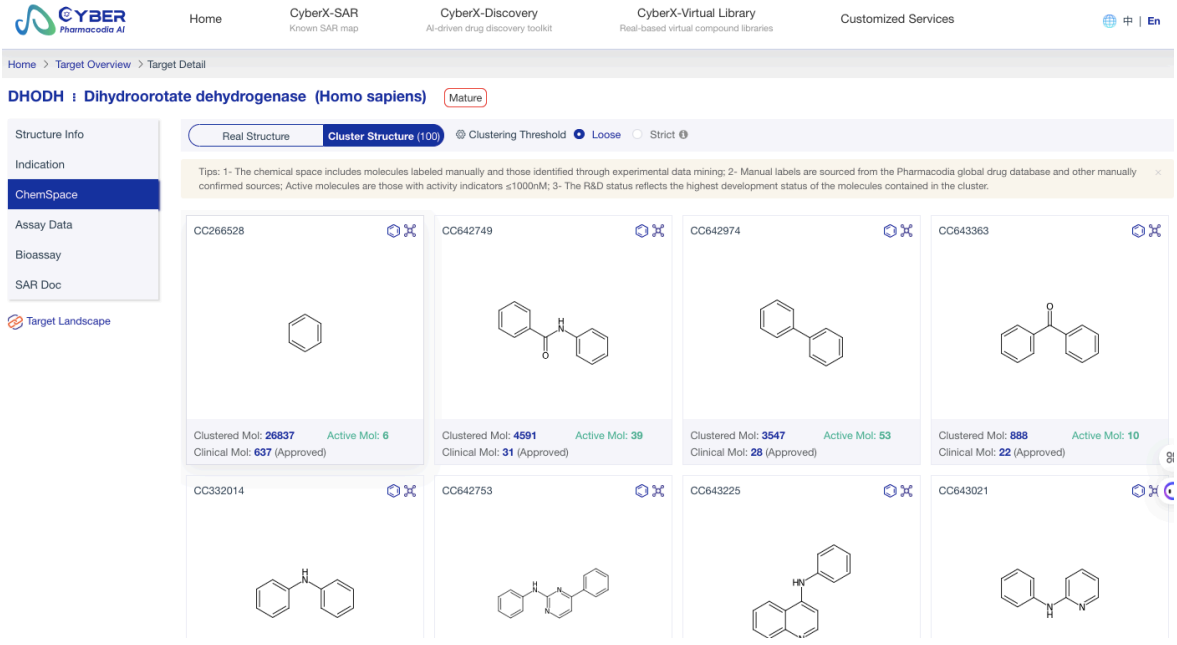

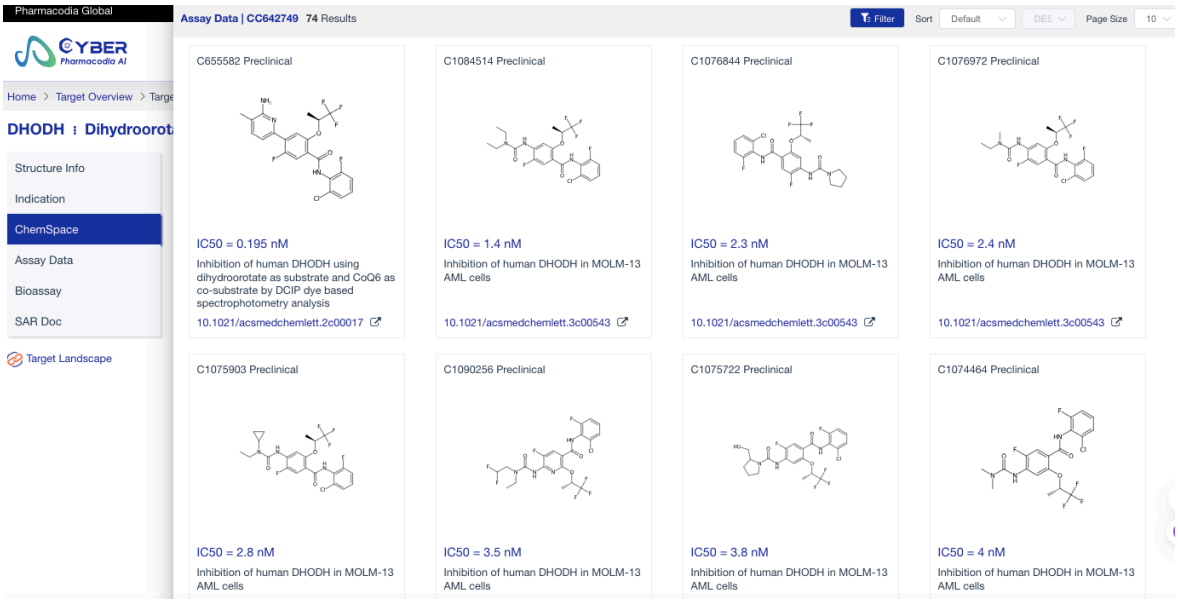

4. Select the "Chemical Space" option tab under the "Chemical Space" option tab in the target interface, and the molecules with DHODH (Homo sapiens) related experimental test activity in the literature included in the CyberSAR platform can be displayed in the form of "R&D stage timeline". Among them, "data mining" highlighted in green font is potential Hit.

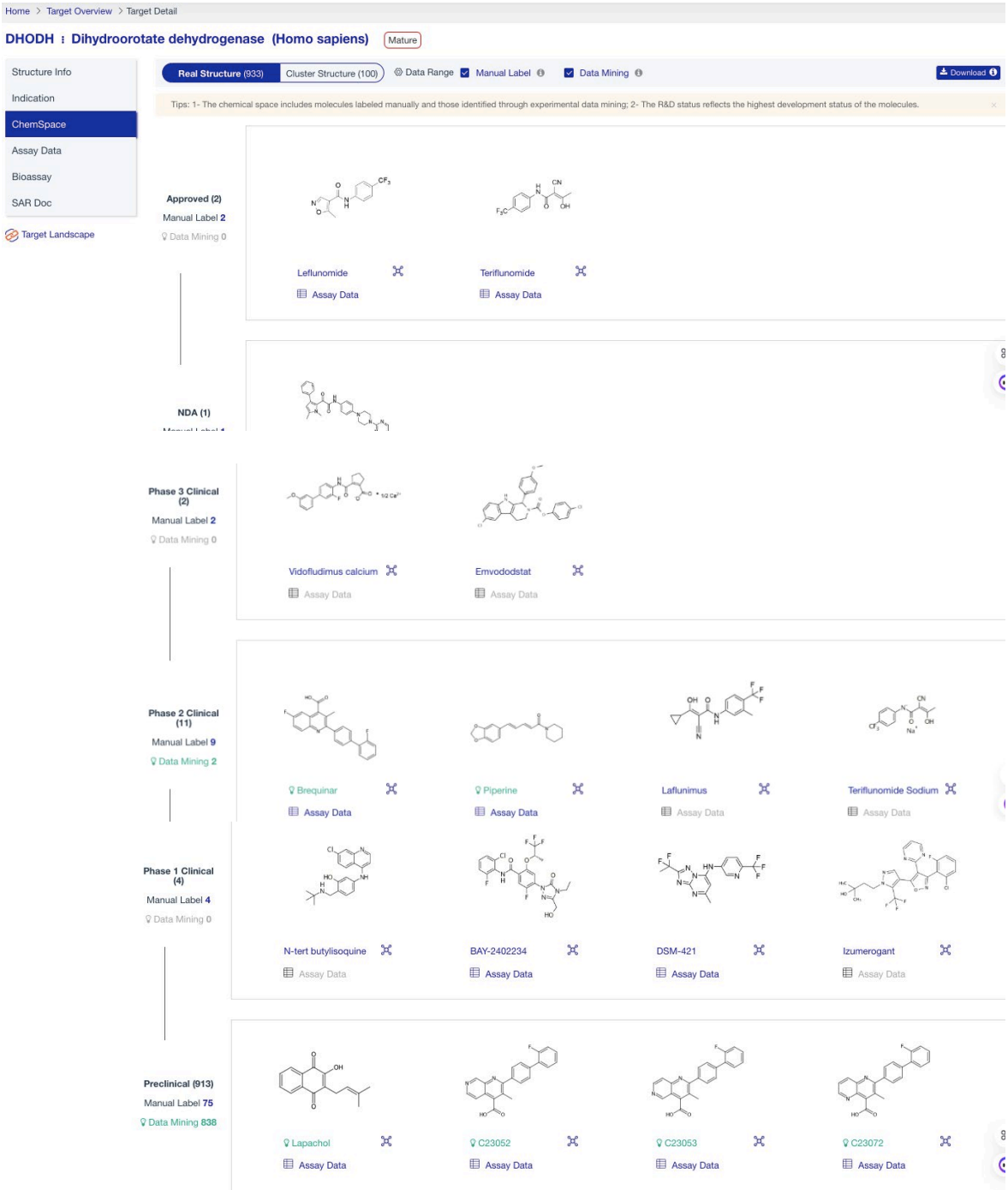

To Explore Cyber-AIDD further Login on your computer using the below Link
https://cyber.pharmacodia.com/#/homePage

If you need further assistance contact us,

For a free trial, Contact Us on

Anil Ranadev
+91 9742627845
anil_ranadev@saspinjara.com

Aravind
+91 9619076286
aravind.p@saspinjara.com

Sachin Marihal
+91 9538033363
sacin.marihal@saspinjara.com

Chetan S
+91 7022031061
chetans@saspinjara.com